The *myeloid/lymphoid leukemia* (*MLL*) gene is located at 11q23, a site frequently involved in chromosomal translocations that occur in aggressive human lymphoid and myeloid leukemias. MLL-AF4 acute lymphoblastic leukemia (ALL) is associated with steroid resistance, has a poor prognosis (24, 25), and is associated with "lineage fragility." MLL-AF4 ALL often expresses both B-cell and monomyelocytic surface antigens; hence, it is often described as "biphenotypic" leukemia. This characteristic suggests that early hematopoietic progenitors are transformed in MLL-AF4 ALL.

A recent survey of miRNAs in ALL showed that miRNA expression patterns differ among ALL subtypes (13). We analyzed publicly available raw data (www.broad.mit.edu/mpr/publications/projects/microRNA/ALL.gct) and discovered that many miRNAs were down-regulated in ALL with *MLL* rearrangements, compared with ALL that do not harbor *MLL* rearrangements (26). Importantly, some miRNAs that have been reported to be tumor suppressors were down-regulated to considerable degrees, raising the question whether these miRNAs are involved in the biology of *MLL*-rearranged ALL, especially in regard to its lineage fragility.

Here, we focused on miR-126, which is down-regulated in *MLL*-rearranged ALL compared with other types of ALL. Through gain- and loss-of-function experiments, we showed that miR-126 positively regulated B-cell fate without affecting expression of EBF1, E2A, and PAX5 by targeting insulin regulatory subunit-1 (IRS-1). Most importantly, miR-126 could partly rescued failed B-cell development in EBF1-deficient hematopoietic progenitor cells (HPCs). Our results elucidate a unique mechanism involved in cell fate, which can partially rescue B lymphopoiesis in EBF1 deficiency.

## Results

**miR-126 Is Down-Regulated in MLL-AF4 ALL, Compared with Other Types of ALL.** We analyzed publicly available raw data (www.broad.mit.edu/mpr/publications/projects/microRNA/ALL.gct) and found that in *MLL*-rearranged ALL, many miRNAs were down-regulated, compared with other types of ALL (13, 26). Of the 10 miRNAs that showed the most dramatic down-regulation, we chose to further analyze miR-126, which has been reported to have tumor-suppressive activity in lung cancer (27) (Fig. 1*A*). We also analyzed other previously published raw data (28) and found that miR-126 is gradually down-regulated during B-cell differentiation (Fig. 1*B*). This result was confirmed by real-time PCR analysis of miR-126 expression in $CD43^+B220^+$, $CD43^-B220^+$, and $IgM^+B220^+$ mouse bone marrow (BM) cells, which correspond to proB, preB, and mature B cells, respectively (Fig. 1*C*). Therefore, we hypothesized that miR-126 is a tumor suppressive miRNA and potential regulator of B-cell development.

**miR-126 Shifts the Balance of B-Cell/Monomyeloid Differentiation Toward B Cells in MLL-AF4 ALL Cells.** To explore the role of miR-126 in hematopoietic cells, we designed a retroviral vector that expresses the miRNA gene together with GFP. The vector was transduced, via retroviral infection, into SEM cells established from an MLL-AF4 ALL patient. In agreement with the observations from other *MLL*-rearranged ALL cell lines, SEM cells endogenously express mature miR-126 at a low level (29).

To examine the functions of miR-126, we overexpressed it in SEM cells. The expression level of mature miR-126 was more than 600-times higher in miR-126–transduced cells than in control cells (29).

SEM cells were transduced with retrovirus vectors expressing either let-7b, miR-126, miR-128b, or no miRNA (negative control). The transduced cells were sorted for those expressing GFP (a marker gene on all of the retroviral vectors) and cultured in RPMI containing 10% (vol/vol) FCS. At 8 wk posttransduction, a significant up-regulation of CD20 (~16%) and CD19 (mean fluorescence intensity, ~600) was observed in SEM cells expressing miR-126, but control cells or cells expressing let-7b or miR-128b showed ~1–2% $CD20^+$ cells and a mean-fluorescence intensity of CD19 expression of 350–450 (Fig. 2). Furthermore, suppression of miR-126 promoted the differentiation of SEM cells into myeloid cells, inducing the down-regulation of CD19 and up-regulation of CD15 (Fig. S1). Accordingly, gain- and loss-of-function experiments in a cell line derived from an MLL-AF4 ALL patient suggested that miR-126 drives B-cell myeloid biphenotypic leukemia differentiation toward B cells, at the expense of myeloid cells.

**miR-126 Shifts the Balance of B-Cell/Monomyeloid Differentiation Toward B Cells Without Up-Regulating Transcription Factors Critical for B-Cell Development.** To confirm that miR-126 affects B-cell development beyond regulating the expression of CD19, CD20, and CD15, we performed a comprehensive analysis of the mRNA transcripts that were up-regulated or down-regulated in SEM cells that expressed miR-126. Using Agilent gene-expression arrays, we identified a set of B-cell genes and a set of monomyeloid genes, as defined by IPA software (Ingenuity Systems). B-cell genes in $miR\text{-}126^+$ SEM cells were significantly up-regulated compared with those in control SEM cells, but the monomyelocyte genes were not (Fig. 3 *A* and *B*, and Dataset S1). These results suggest that miR-126–expressing SEM cells up-regulated not only CD20 and CD19 but also the global expression of other B-cell genes in SEM cells. We concluded that miR-126 shifted the balance of B-cell/monomyeloid differentiation toward B cells in MLL-AF4 ALL cells. Interestingly, PAX5, EBF1, and E2A, critical transcription factors in B-lymphopoiesis, were not up-regulated. Instead, E2A was slightly down-regulated in miR-126–expressing cells (Fig. 3*C*). Expressions of non–B-cell genes targeted by E2A, EBF1, or PAX5 were not altered by the transduction of miR-126 (Figs. S2 and S3, and Dataset S2). This finding suggests that neither transcriptional nor functional activity of PAX5, EBF1, and

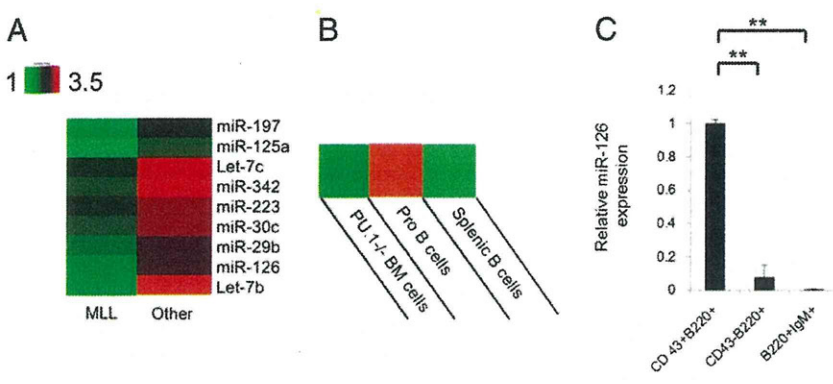


**Fig. 1.** Expression of miR-126 in acute lymphocytic leukemia and mouse hematopoietic cells. (*A*) The miRNAs that are most highly down-regulated in *MLL*-rearranged ALL compared with other types of ALL. These data were previously published and were reanalyzed here and presented as a heat map. (*B*) Expression of miR-126 in $PU.1^{-/-}$ BM cells, BM proB cells, and splenic B cells. These data were previously published and were reanalyzed here and presented as a heat map. (*C*) miRNA expression normalized by U6 expression in B-cell precursors detected by quantitative RT-PCR. B-cell precursor cells at various stages of differentiation were isolated from BM ($n$ = 3) by FACS. ProB cells, $B220^+CD43^+IgM^-$; PreB cells, $B220^+CD43^-IgM^-$; immature B cells, $B220^+CD43^-IgM^+$. $^{**}P < 0.05$.

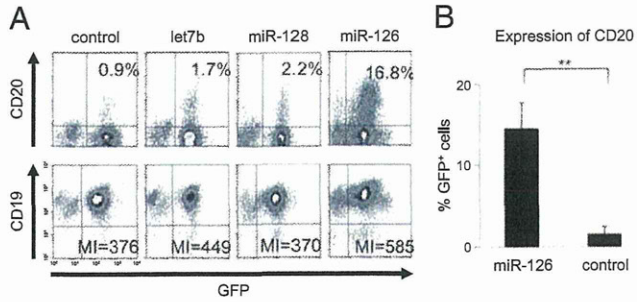


**Fig. 2.** Induction of B-cell differentiation by miR-126. (*A*) Representative flow plots of sorted SEM cells transduced with control, let-7b, miR-128b, or miR-126 vectors. The pregated live cells were analyzed. MI, mean intensity. (*B*) Percentages of $CD20^+$ cells among miR-126 or control vector-transduced SEM cells ($n = 3$).

E2A are enhanced by miR-126. Therefore, the shift toward B-cell lineage might be independent of PAX5, EBF1, and E2A.

**miR-126 Regulates Lineage Fate in Lymphoid-Myeloid Progenitor Cells.** To further analyze the B-cell differentiation caused by miR-126, we studied the effects of miR-126 transduction in a bilineage primary cell culture system. Mouse $Lin^-$ HPCs isolated from fetal liver (FL), when cultured on thymic stromal (TSt)-4 cells, differentiate into monomyelocytic cells and B cells in vitro. This system allowed us to quantify the proportion of B cells and monomyelocytic cells derived from HPCs (30) following the perturbation of miR-126 expression. We transduced $Lin^-$ cells with a retroviral construct harboring miR-126 or a control miRNA, and cultured them on TSt-4 cells. Then B cells were enumerated by flow cytometric analysis of the $CD19^+$ population. On day 5, in contrast to the control $Lin^-$ cells, miR-126–expressing cells yielded an average fourfold enrichment of B cells (Fig. 4 *A* and *B*), and the proportion of $mac1^+$ monomyelocytic cells showed a reciprocal reduction (Fig. 4*B*). This result indicates that miR-126 shifts the balance of B-cell/monomyeloid differentiation toward B cells in normal HPCs.

To clarify which progenitor populations of $Lin^-$ cells were affected by miR-126, we fractionated $Lin^-$ cells into three groups: $Lin^-Flt3^+c\text{-}Kit^+Sca1^+IL\text{-}7R^-$ cells, $Lin^-c\text{-}Kit^{low}Sca1^{low}IL\text{-}7R^+$ cells, and $Lin^-c\text{-}Kit^+Sca1^-IL\text{-}7R^-$ cells. Although $Lin^-c\text{-}Kit^{low}Sca1^{low}IL\text{-}7R^+$ cells were slightly affected by miR-126, the most dramatic effect of miR-126 was on $Lin^-Flt3^+c\text{-}Kit^+Sca1^+IL\text{-}7R^-$ cells. Forced expression of miR-126 resulted in a statistically significant increase in $CD19^+$ cells in $Lin^-Flt3^+c\text{-}Kit^+Sca1^+IL\text{-}7R^-$ cells (Fig. 4*C* and Fig. S4). Next, we determined whether miR-126 had reprogrammed the myeloid-committed cells into B cells. To address this theory, we transduced miR-126 into $Lin^-c\text{-}Kit^+Sca1^-IL\text{-}7R^-$ cells, the majority of which were committed to the monomyelocyte lineage. miR-126 did not increase the proportion of $Lin^-c\text{-}kit^+Sca1^-IL\text{-}7R^-$ cells that were positive for CD19, indicating that miR-126 cannot reprogram monomyelocyte-committed cells (Fig. 4*C* and Fig. S4). Considering that $Lin^-c\text{-}Kit^{low}Sca1^{low}IL\text{-}7R^+$ cells are lymphoid-restricted progenitor cells, which still have potential to differentiate into myeloid cells although much less so than $Lin^-Flt3^+c\text{-}Kit^+Sca1^+IL\text{-}7R^-$ cells (7), these experiments suggest that miR-126 primarily regulates lymphoid versus myeloid lineage commitment in the multipotent cell population, and does not regulate the expansion of lymphoid- or myeloid-restricted progenitor cells.

**miR-126 Increases B Cells in Vivo.** Having established a functionally important role for miR-126 in an in vitro model of B-cell differentiation, we next examined the function of miR-126 in vivo. The competitive transplantation assays were performed in the Ptprc congenic mouse model, transducing $Ptprc^b$ (CD45.2) or $Ptprc^a$ (CD45.1) $lin^-$ BM hematopoietic stem and progenitor cells, respectively, with either the miR126 or the control vector. The data were published in ref. 31.

Using flow cytometry, we characterized BM cells according to their expression of cell surface markers for B cells (CD19), T cells (CD3), or monomyeloid cells (Mac1). Remarkably, compared with control cells, the BM cells expressing miR-126 exhibited a significant expansion of $CD19^+$ B cells and reduction of $CD3^+$ T cells and $mac\text{-}1^+$ monomyeloid cells in the peripheral blood 4 wk after BM transplantation ($CD19^+$ cell frequency, $45.5 \pm 9.9\%$ vs. $70.7 \pm 05.4\%$; $P < 0.05$; $CD3^+$ cell frequency, $13.3 \pm 5.8\%$ vs. $5.5 \pm 2.0\%$; $P < 0.05$; $mac1^+$ cell frequency, $40.8 \pm 8.5\%$ vs. $23.1 \pm 6.1\%$; $P < 0.05$) (Fig. 5).

**IRS-1 Is a Functional Target of miR-126 During B-Cell Expansion.** The experiments described above establish an important role for miR-126 in B-cell development of HPCs. We next sought to determine the mRNA target of miR-126 that would explain its effect on B-lymphopoiesis. We initially focused on targets that were commonly predicted across multiple sequence-based prediction algorithms (10, 32–34). We chose *IRS-1* as a candidate because its gene expression was reduced in $Lin^-$ FL cells overexpressing miR-126 (Fig. 6 *A* and *B* and Fig. S5). We focused on IRS-1 because it has known functions in cell proliferation and differentiation processes; higher expression of IRS-1 is associated with proliferation, and lower levels are associated with differentiation (35). First, we cloned the *IRS-1* 3′ UTR into a luciferase reporter vector and found that miR-126 repressed reporter activity by more than twofold, consistent with the predicted targeting of IRS-1 by miR-126 (34). This experiment confirmed that miR-126 negatively regulates the mRNA expression level of IRS-1 directly through its 3′ UTR (29). Then, we addressed whether the repression of IRS-1 could explain the B-cell differentiation observed with miR-126 overexpression using the in vitro mouse FL cell coculture system with TSt-4 cells. We tested whether complementation of IRS-1 by exogenous cDNA

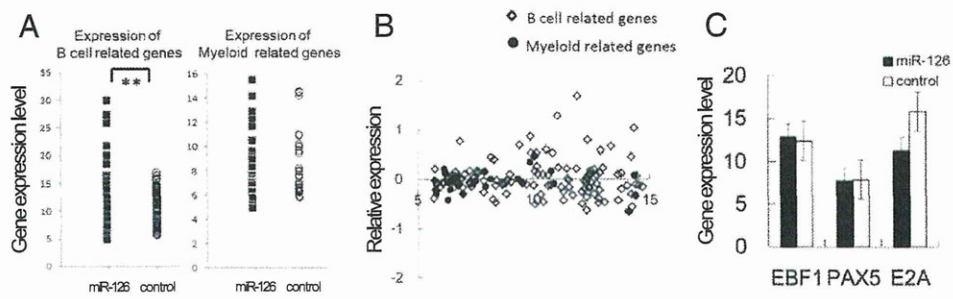


**Fig. 3.** miR-126 induces B-cell differentiation in MLL-AF4 ALL cells without up-regulating EBF1, PAX5, or E2A. (*A*) B-cell–related genes were significantly up-regulated in miR-126–transduced MLL-AF4 ALL cells compared with control-transduced MLL-AF4 ALL cells (*Left*), but monomyelocyte related genes were not (*Right*). The *y* axis shows log-transformed data. (*B*) Intensity scatter plot comparing miRNA profiles in miR-126–transduced and control-transduced MLL-AF4 ALL cells. The *x* axis shows log-transformed data, and the *y* axis shows the log ratio. (*C*) Intensity of E2A, PAX5, or EBF mRNA expression in miR-126– or control-transduced SEM cells. The *y* axis shows log-transformed data.

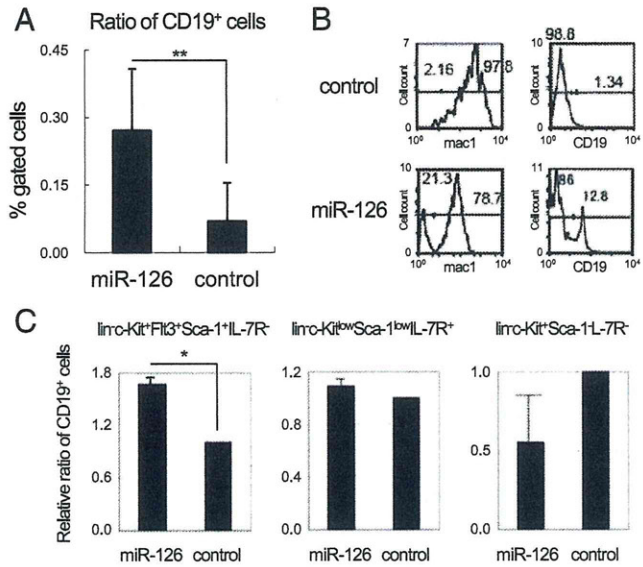


**Fig. 4.** miR-126 increases the proportion of B cells among progenitor FL cells cocultured with TSt-4 cells. Hematopoietic progenitors derived from mouse FL cells were sorted into $Lin^-$ cells and transduced with control and miR-126–expressing viral constructions. The cells were then cocultured with TSt-4 cells to differentiate them into B cells or monocytes and analyzed after 5 d of differentiation using flow cytometric analysis with the lineage markers CD19 (B cells) and mac1 (monocytes). (*A*) Effects of the expression constructs on the percentage of $CD19^+$ cells. Error bars represent SD ($n = 3$). $^{**}P < 0.03$. (*B*) Representative flow histogram of control vector- and miR-126–transduced $Lin^-$ FL cells. Expression of CD19 and mac1 were determined. These plots pregated on $GFP^+$ live cells. (*C*) Hematopoietic progenitors derived from mouse FL cells were sorted into $Lin^-Flt3^+c\text{-}Kit^+Sca1^+IL\text{-}7R^-$ cells, $Lin^-c\text{-}Kit^{low}Sca1^{low}IL\text{-}7R^+$ cells, and $Lin^-c\text{-}Kit^+Sca1^-IL\text{-}7R^-$ cells and transduced with control and miR-126-expressing viral constructs. Then, the cells were cocultured with TSt-4 cells to differentiate them into B cells or monocytes and analyzed by flow cytometry after 5 d of differentiation for the lineage markers CD19 (B cells). Effects of the expression constructs on the percentage of $CD19^+$ cells. The *y* axis represents the $CD19^+$ miR-126 transduced cells relative to the control. The error bars indicate SD ($n = 3$). $^*P < 0.03$.

that is not affected by miR-126 could reverse the observed increase in B-cell differentiation. Murine stem cell virus-based constructs containing the *IRS-1* coding sequence were generated with human nerve growth factor receptor (NGFR). Then, the IRS-1 coding sequence or a control vector was cotransduced with miR-126 into $Lin^-$ cells to see whether IRS-1 expression could rescue the miR-126 phenotype. As shown in Fig. 6 *C* and *D*, $CD19^+$ B cells accounted for 2.34% of the 11.8% of $Lin^-$ FL cells transduced with IRS-1 and miR-126, and 36.2% of the 56% cells transduced with control vector and miR-126. A total of 20% of IRS-1- and miR-126–transduced $Lin^-$ FL cells and 70% of control vector- and miR-126–transduced cells were $CD19^+$, indicating that there were significantly fewer $CD19^+$ B cells among IRS-1–transduced $Lin^-$ FL cells than among control cells (Fig. 6*D*). The opposite results were obtained for $mac1^+$ monomyelocytic cells (Fig. 6 *C* and *D*). These findings indicate that the influence of miR-126 on B-cell differentiation was abrogated by the introduction of IRS-1 lacking its 3′ UTR in murine FL cells, suggesting that the target genes of miR-126 in this system include *IRS-1*.

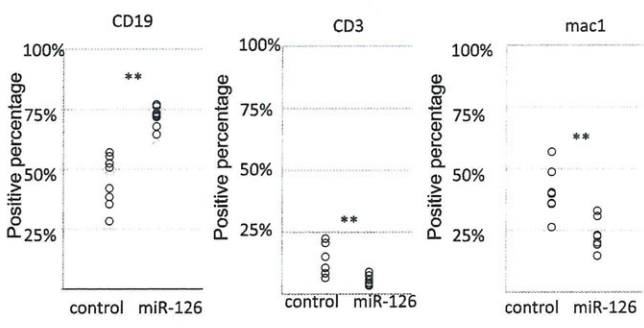


**Fig. 5.** miR-126 induces B-cell expansion in vivo. The competitive transplantation assays were performed in the Ptprc congenic mouse model, transducing $Ptprc^b$ (CD45.2) or $Ptprc^a$ (CD45.1) $lin^-$ BM hematopoietic stem and progenitor cells, respectively, with either the miR126 or the control vector. The peripheral blood of recipient mice were analyzed 4 wk post-transplantation, when the hematopoietic system had largely recovered in the hosts. The data were published previously (31). Each dot represents data from one recipient mouse. $^{**}P < 0.01$.

**miR-126 Can Rescue Failed B-Cell Differentiation in EBF1-Deficient HPCs.** Mice lacking EBF1 fail to express most B-cell genes, including Cd79a and Cd79b, and do not undergo Igh V-to-DJ recombination in the BM. Neither E2A nor PAX5, which are critical transcriptional factors, can rescue the failure in EBF1-deficient HPCs. Ectopic expression of EBF1 is able to rescue B-lymphopoiesis in multipotent progenitors blocked at earlier stages of development because of targeted deletion of key lymphoid transcription factors such as E2A, PU.1, and PAX5. Taken together, these data indicate that EBF1 is an essential specification factor for the B-cell lineage. Accordingly, we tested whether failure of B-cell development because of EBF1 deficiency, can be rescued by miR-126. miR-126 induces B-cell differentiation in MLL-AF4 ALLs without affecting EBF1, PAX5, and E2A, suggesting that it may potentially induce B-cell differentiation by an alternative mechanism to transcriptional factors. We established EBF1-deficient HPCs expressing low amounts of B220 but not CD19. Retrovirus-mediated expression of miR-126 in these cells markedly up-regulated B220, but not CD19 (Fig. 7*A*). CD19 expression is contingent on EBF1. In the BM, B220 is up-regulated during the maturation of prepro B cells into mature B cells (36). Moreover, expression of B-cell genes, such as PAX5, CD79a/b, and recombination activating gene (RAG)1/2, is up-regulated (Fig. 7*B*). Although RAG1/2 was up-regulated by miR-126, V-DJ rearrangements were not induced by miR-126. miR-126 affected not only gene expression profiles, but the growth of EBF1-deficient HPCs. Although the proportion of control vector-carrying EBF1-deficient HPCs gradually decreased during 28-d culture, the proportion of EBF1-deficient HPCs carrying miR-126 increased (Fig. 7*C*). This finding suggested miR-126 promoted the proliferation or survival of EBF1-deficient HPCs. Next, we calculated the doubling time of them. The doubling time of control EBF1-deficient HPCs ($26.6 \pm 1.5$ h) was comparable to that of the original EBF1-deficient HPCs ($27.0 \pm 2.0$ h). In contrast, the doubling time of miR-126-transduced EBF1-deficient HPCs ($21.4 \pm 1.0$ h) was significantly shorter than that of control cells. This result indicates that miR-126 enhanced the proliferation of EBF1-deficient HPCs. These results suggest that miR-126 can partly rescue failed B-cell lineage development and specification because of EBF1 deficiency.

## Discussion

We found that miR-126 was down-regulated in MLL-AF4 ALL, a cancer with an immature B-cell phenotype, compared with other types of ALL. Furthermore, miR-126 expression strikingly decreased during successive stages of B-cell maturation in the BM, suggesting that this miRNA may participate in early B lymphopoiesis, and deregulation of its expression is involved in leukemogenesis. Indeed, inducing the re-expression of miR-126 promoted B-cell development in MLL-AF4 ALL, the mouse FL, and BM hematopoietic cells. miR-126, which was ectopically expressed in preB and immature B cells, did not affect B-cell

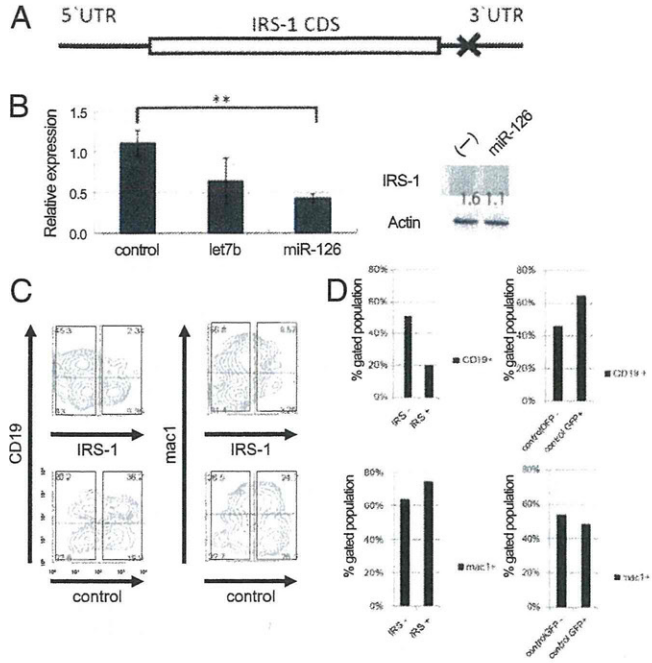


**Fig. 6.** IRS-1 is a functional target of miR-126 during B-cell expansion. (*A*) Location of the predicted (Pictar) miR-126 target sequence (X) in the 3′ UTR of the human IRS-1 mRNA. (*B*) Relative expression of IRS-1 mRNA normalized to U1A expression by quantitative PCR analysis of Lin$^-$ FL cells overexpressing miR-126, let-7, or control vector ($n$ = 3, *Left*). $^{**}P < 0.05$. Western blot analysis of IRS-1 was performed with total protein extracts of miR-126–overexpressing or control Lin$^-$ FL cells (*Right*). The relative intensity of each band (indicated below the bands) was determined using Multigauge software and normalized to the GAPDH loading control. (*C* and *D*) Ectopic expression of IRS-1 in miR-126-expressing Lin$^-$ FL cells decreases B-cell numbers. (*C*) Representative plots for CD19 and mac1 expression in IRS-1$^+$/IRS-1$^-$ miR-126$^+$ and controlGFP$^+$/controlGFP$^-$ miR-126$^+$ Lin$^-$ FL cells. (*D*) Percentage of CD19$^+$ or mac1$^+$ cells in pregated IRS1$^+$, IRS1$^-$, control$^+$, or control$^-$ cells. Square indicates each pregated cells.

maturation, suggesting that its effect was limited to early B-cell development. Its effect was most dramatically observed in Lin$^-$c-Kit$^+$Sca1$^+$ uncommitted progenitor cells in the FL, suggesting miR-126 is involved in cell fate regulation. Notably, even though the expression of key transcription factors in B-cell development; E2A, EBF, and PAX5, were unchanged in miR-126–expressing cells, miR-126 plays a critical role in regulating the differentiation of B cells in leukemia, in which the deregulation of differentiation because of dysfunction of transcription factors is supposed to be involved in leukemogenesis (37). Moreover, expression of miR-126 in EBF1-deficient HPCs partly rescued B-lymphopoiesis, leading to the up-regulation of several B-cell genes and enhanced proliferation. Importantly, CD79a, which is critically regulated by EBF1, was up-regulated by miR-126 in EBF1-deficient cells. The stepwise expression and function of several factors is involved in cell fate determination. EBF1 can rescue B-cell development in E2A-, PU.1-, and PAX5-deficient hematopoietic stem cells. Conversely, these transcriptional factors cannot rescue B-cell development, indicating that EBF1 controls the minimal essential system for B-cell development. Our finding that miR-126 partly rescued B-cell development in EBF1-deficient HPCs suggests that miR-126, which is not a transcriptional factor, has critical roles in B-cell development. However, miR-126 is dispensable for B-cell development, because miR-126 deficiency does not cause any defects in B-lymphopoiesis. Taken together, our observations lead us to conclude that miR-126–mediated B-cell differentiation is at least partly independent of canonical assembly of a transcriptional factor regulatory network. miR-126 has the potential to compensate for the deregulation of cell fate caused by dysfunction of transcription factors in leukemia and is critically involved in B-cell lineage specification. These results challenge the view that miRNAs merely play fine-tuning roles in establishing lineage fate (8).

Surveying the predicted targets of miR-126, we found several genes that play important roles in myeloid development, including *IRS-1*, *v-crk sarcoma virus CT10 oncogene homolog* (*CRK*), and *homeobox A9* (*HOXA9*). Two highly conserved 8-nt sites in the 3′ UTR of IRS-1 mRNA, one conserved 7-nt site in the CRK 3′ UTR, and one conserved 7-nt site in the HOXA9 3′ UTR are complementary to the miR-126 "seed" region. Among these targets, we demonstrated that miR-126 targets IRS-1 during B-cell differentiation. IRS-1 is the main docking protein of both type 1 insulin-like growth factor I receptor and the insulin receptor. IRS-1 is a principal substrate of the insulin receptor tyrosine kinase. IRS-1 undergoes multisite tyrosine phosphorylation and mediates insulin signaling by associating with various signaling molecules containing Src homology 2 domains (38). Overexpression of *IRS-1* inhibits differentiation and promotes transformation of hematopoietic cells into a tumor-forming cell line (35). Although the function of IRS-1 in B-cell development has yet to be determined, it is reasonable that IRS-1, an inhibitor of differentiation, is down-regulated by miR-126 during B-cell differentiation.

Future investigations exploring the regulation of miR-126 expression are needed to understand its function; its expression is known to be greatest in highly vascularized tissues, such as the lung, heart, and kidney (39–41), and is also present in bronchial epithelium (27). miR-126 is located on chromosome 9q34.3 and is encoded within intron 5 of *epidermal growth factor like-7* (39). Recently, miR-126 was shown to function in angiogenesis, as miR-126–deficient mice are embryonic lethal because of vascular malformation (42). In the hematopoietic system, Landgraf et al. (43) reported qualitative detection of miR-126 in the CD34$^+$ pool containing hematopoietic stem cells, but they did not examine the function of miR-126 in this cell population. miR-126 has also

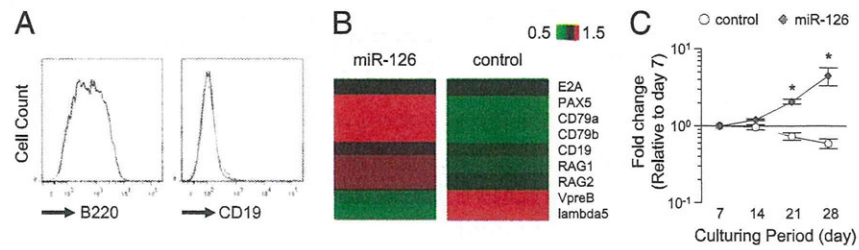


**Fig. 7.** miR-126 up-regulates B-cell markers and promotes cell proliferation in EBF1-deficient HPCs. (*A*) HPC lines derived from EBF1-deficient mouse FL were transduced with control and miR-126–expressing viral constructs. Cells were cocultured with TSt-4 cells in the presence of IL-7, stem cell factor, and Flt3 ligand and analyzed after 10 d of differentiation by flow cytometry for the B-cell lineage markers B220 and CD19. The black and gray lines indicate miR-126 and control vector-transduced pregated live cells, respectively. The same results were obtained three times. (*B*) cDNA analysis of B-lineage gene expression in the HPC lines derived from EBF1-deficient HPCs transduced with a viral construct expressing miR-126 (*Left*) or a control vector (*Rght*). (*C*) The proportion of miR-126–transduced EBF1-deficient HPCs in culture gradually increases, but that of control vector-transduced cells does not. The proportions of vector-carrying EBF1-deficient HPCs are shown as fold changes relative to day 7. $^*P < 0.05$.

been reported to be down-regulated during terminal megakaryocytopoiesis and up-regulated in megakaryocytic cell lines (44). We and others have found that miR-126 is down-regulated in B-cell differentiation. The regulation of miR-126 expression should be further investigated.

Finally, the observed function of miR-126 as an inducer of differentiation suggests miR-126 might be a promising therapeutic target. In acute promyelocytic leukemia, retinoic acid induces terminal differentiation of leukemic cells. This "differentiation induction" therapy has been tried in many types of tumors without much success. miR-126 may be an agent for differentiation induction therapy for ALL; thus, further studies are needed to evaluate its potential as a differentiation inducer.

## Materials and Methods

**Ebf1$^{-/-}$ Progenitor Cells.** *Ebf1*$^{-/-}$ hematopoietic progenitor (Lin$^-$) cells were isolated from the *Ebf1*$^{-/-}$ livers of 14 d postcoitum embryos and cultured on TSt-4 stromal cells in IMDM containing 10% (vol/vol) FCS, 2-ME ($5 \times 10^{-5}$ M), penicillin (10 U/mL), and streptomycin (10 μg/mL) in the presence of stem cell factor, IL-7, and Flt3 ligand (10 ng/mL each), as described previously (45, 46).

**Gene-Expression Analysis.** RNA from cells used for microarray analysis was isolated using the RNeasy Mini Kit (Qiagen). For microarray analysis, splenocytes were cultured for 72 h with or without 10 μM IM. Gene-expression microarray analysis was performed using two-color microarray-based gene-expression analysis (Agilent Technologies) according to the manufacturer's instructions. After scanning, expression values for the genes were determined using GeneSpringGX software. All experiments were done in the duplicates.

**Western Blot Analysis.** FL cells transduced with either control or miR-126 vector were lysed in sample loading buffer and separated by SDS/PAGE and transferred to a polyvinylidene fluoride membrane. The membrane was incubated with primary antibody against IRS-1 (Cell Signaling Technology), followed by peroxidase-conjugated anti-rabbit Ig (GE Healthcare).

**BM Transplantation.** Lin- BM cells from congenic mice (Ptprca and Ptprcb, respectively) were transduced with a 126OE vector or with a CTRL vector, and injected in a 1:1 ratio into myeloablated recipients (31).

Peripheral blood analysis was performed 4 wk after the BM transplantation. Mononuclear cells were stained with various antibodies and analyzed on a FACSCalibur flow cytometer (BD Biosciences) and using FlowJo software (Tree Star).

**Antibodies.** Antibodies specific for CD3, CD19, CD20, Mac1, Gr-1, Flt3, c-kit, Sca1, and IL-7Rα were purchased from eBioscience.

Primer sequences, reagents, and more detailed methods are shown in *SI Materials and Methods*.

**ACKNOWLEDGMENTS.** We thank Mr. Keisuke Takahashi, and Drs. Masayuki Tanaka and Hideki Hayashi for technical assistance. We also thank Drs. Yoshio Katayama and Mari Sato for technical advice. This work was supported by the Japan Society for the Promotion of Science (to A.K.).

1. Cantor AB, Orkin SH (2002) Transcriptional regulation of erythropoiesis: An affair involving multiple partners. *Oncogene* 21(21):3368–3376.
2. Friedman AD (2002) Transcriptional regulation of myelopoiesis. *Int J Hematol* 75(5): 466–472.
3. Ye M, Graf T (2007) Early decisions in lymphoid development. *Curr Opin Immunol* 19(2):123–128.
4. Zhu J, Emerson SG (2002) Hematopoietic cytokines, transcription factors and lineage commitment. *Oncogene* 21(21):3295–3313.
5. Pongubala JM, et al. (2008) Transcription factor EBF restricts alternative lineage options and promotes B cell fate commitment independently of Pax5. *Nat Immunol* 9(2): 203–215.
6. Zheng W, Flavell RA (1997) The transcription factor GATA-3 is necessary and sufficient for Th2 cytokine gene expression in CD4 T cells. *Cell* 89(4):587–596.
7. Xie H, Ye M, Feng R, Graf T (2004) Stepwise reprogramming of B cells into macrophages. *Cell* 117(5):663–676.
8. Bartel DP (2004) MicroRNAs: Genomics, biogenesis, mechanism, and function. *Cell* 116(2):281–297.
9. Bagga S, et al. (2005) Regulation by let-7 and lin-4 miRNAs results in target mRNA degradation. *Cell* 122(4):553–563.
10. Lewis BP, Burge CB, Bartel DP (2005) Conserved seed pairing, often flanked by adenosines, indicates that thousands of human genes are microRNA targets. *Cell* 120(1): 15–20.
11. Miranda KC, et al. (2006) A pattern-based method for the identification of MicroRNA binding sites and their corresponding heteroduplexes. *Cell* 126(6):1203–1217.
12. Ambros V (2004) The functions of animal microRNAs. *Nature* 431(7006):350–355.
13. Lu J, et al. (2005) MicroRNA expression profiles classify human cancers. *Nature* 435(7043):834–838.
14. Volinia S, et al. (2006) A microRNA expression signature of human solid tumors defines cancer gene targets. *Proc Natl Acad Sci USA* 103(7):2257–2261.
15. Xiao C, et al. (2007) MiR-150 controls B cell differentiation by targeting the transcription factor c-Myb. *Cell* 131(1):146–159.
16. Chen CZ, Li L, Lodish HF, Bartel DP (2004) MicroRNAs modulate hematopoietic lineage differentiation. *Science* 303(5654):83–86.
17. Li QJ, et al. (2007) miR-181a is an intrinsic modulator of T cell sensitivity and selection. *Cell* 129(1):147–161.
18. Zhou B, Wang S, Mayr C, Bartel DP, Lodish HF (2007) miR-150, a microRNA expressed in mature B and T cells, blocks early B cell development when expressed prematurely. *Proc Natl Acad Sci USA* 104(17):7080–7085.
19. Johnson SM, et al. (2005) RAS is regulated by the let-7 microRNA family. *Cell* 120(5): 635–647.
20. Johnson CD, et al. (2007) The let-7 microRNA represses cell proliferation pathways in human cells. *Cancer Res* 67(16):7713–7722.
21. Metzler M, Wilda M, Busch K, Viehmann S, Borkhardt A (2004) High expression of precursor microRNA-155/BIC RNA in children with Burkitt lymphoma. *Genes Chromosomes Cancer* 39(2):167–169.
22. He L, et al. (2005) A microRNA polycistron as a potential human oncogene. *Nature* 435(7043):828–833.
23. Costinean S, et al. (2006) Pre-B cell proliferation and lymphoblastic leukemia/high-grade lymphoma in E(mu)-miR155 transgenic mice. *Proc Natl Acad Sci USA* 103(18): 7024–7029.
24. Pui CH, et al. (2003) Clinical heterogeneity in childhood acute lymphoblastic leukemia with 11q23 rearrangements. *Leukemia* 17(4):700–706.
25. Pieters R, et al. (2007) A treatment protocol for infants younger than 1 year with acute lymphoblastic leukaemia (Interfant-99): An observational study and a multicentre randomised trial. *Lancet* 370(9583):240–250.
26. Kotani A, et al. (2009) miR-128b is a potent glucocorticoid sensitizer in MLL-AF4 acute lymphocytic leukemia cells and exerts cooperative effects with miR-221. *Blood* 114(19):4169–4178.
27. Crawford M, et al. (2008) MicroRNA-126 inhibits invasion in non-small cell lung carcinoma cell lines. *Biochem Biophys Res Commun* 373(4):607–612.
28. Monticelli S, et al. (2005) MicroRNA profiling of the murine hematopoietic system. *Genome Biol* 6(8):R71.
29. Harnprasopwat R, et al. (2010) Alteration of processing induced by a single nucleotide polymorphism in pri-miR-126. *Biochem Biophys Res Commun* 399(2):117–122.
30. Lu M, Kawamoto H, Katsube Y, Ikawa T, Katsura Y (2002) The common myelolymphoid progenitor: a key intermediate stage in hemopoiesis generating T and B cells. *J Immunol* 169(7):3519–3525.
31. Lechman ER, et al. (2012) Attenuation of miR-126 activity expands HSC in vivo without exhaustion. *Cell Stem Cell* 11(6):799–811.
32. Krek A, et al. (2005) Combinatorial microRNA target predictions. *Nat Genet* 37(5): 495–500.
33. Xie X, et al. (2005) Systematic discovery of regulatory motifs in human promoters and 3′ UTRs by comparison of several mammals. *Nature* 434(7031):338–345.
34. Zhang J, et al. (2008) The cell growth suppressor, mir-126, targets IRS-1. *Biochem Biophys Res Commun* 377(1):136–140.
35. Prisco M, et al. (2004) Role of pescadillo and upstream binding factor in the proliferation and differentiation of murine myeloid cells. *Mol Cell Biol* 24(12):5421–5433.
36. Stehling-Sun S, Dade J, Nutt SL, DeKoter RP, Camargo FD (2009) Regulation of lymphoid versus myeloid fate 'choice' by the transcription factor Mef2c. *Nat Immunol* 10(3):289–296.
37. Gilliland DG (2002) Molecular genetics of human leukemias: New insights into therapy. *Semin Hematol* 39(4, Suppl 3)6–11.
38. Myers MG, Jr., Sun XJ, White MF (1994) The IRS-1 signaling system. *Trends Biochem Sci* 19(7):289–293.
39. Baskerville S, Bartel DP (2005) Microarray profiling of microRNAs reveals frequent coexpression with neighboring miRNAs and host genes. *RNA* 11(3):241–247.
40. Harris TA, Yamakuchi M, Ferlito M, Mendell JT, Lowenstein CJ (2008) MicroRNA-126 regulates endothelial expression of vascular cell adhesion molecule 1. *Proc Natl Acad Sci USA* 105(5):1516–1521.
41. Wang Y, et al. (2007) Identification of rat lung-specific microRNAs by micoRNA microarray: Valuable discoveries for the facilitation of lung research. *BMC Genomics* 8:29.
42. Wang S, et al. (2008) The endothelial-specific microRNA miR-126 governs vascular integrity and angiogenesis. *Dev Cell* 15(2):261–271.
43. Landgraf P, et al. (2007) A mammalian microRNA expression atlas based on small RNA library sequencing. *Cell* 129(7):1401–1414.
44. Garzon R, et al. (2006) MicroRNA fingerprints during human megakaryocytopoiesis. *Proc Natl Acad Sci USA* 103(13):5078–5083.
45. Ikawa T, Kawamoto H, Wright LY, Murre C (2004) Long-term cultured E2A-deficient hematopoietic progenitor cells are pluripotent. *Immunity* 20(3):349–360.
46. Lin YC, et al. (2010) A global network of transcription factors, involving E2A, EBF1 and Foxo1, that orchestrates B cell fate. *Nat Immunol* 11(7):635–643.

G Model
IJP-13419; No. of Pages 8
ARTICLE IN PRESS

International Journal of Pharmaceutics xxx (2013) xxx–xxx

Contents lists available at SciVerse ScienceDirect

International Journal of Pharmaceutics

journal homepage: www.elsevier.com/locate/ijpharm

# A versatile drug delivery system using streptavidin-tagged pegylated liposomes and biotinylated biomaterials

Ming-Han Chen[a,b,1], Yasushi Soda[c,1], Kiyoko Izawa[d], Seiichiro Kobayashi[d], Kenzaburo Tani[e], Kazuo Maruyama[f], Arinobu Tojo[d], Shigetaka Asano[g,*]

[a] Department of Medicine, National Yang-Ming University Hospital, I-Lan, Taiwan
[b] Department of Medicine, National Yang-Ming University, Taipei, Taiwan
[c] Laboratory of Genetics, Salk Institute for Biological Studies, La Jolla, CA, USA
[d] Division of Molecular Therapy, Advanced Clinical Research Center, Institute of Medical Science, University of Tokyo, Tokyo, Japan
[e] Division of Molecular and Clinical Genetics, Department of Molecular Genetics, Medical Institute of Bioregulation, Kyushu University, Fukuoka, Japan
[f] Department of Drug Delivery Research, Liposome Technology for DDS and Immunology, Faculty of Pharma-Sciences, Teikyo University, Tokyo, Japan
[g] Department of Chemistry/Biological Chemistry, School of Science and Engineering, Waseda University, Tokyo, Japan

ARTICLE INFO

*Article history:*
Received 12 January 2013
Received in revised form 8 May 2013
Accepted 13 June 2013
Available online xxx

*Keywords:*
Drug delivery system
Immunoliposome
Tumor-targeting
Internalization
Streptavidin
Biotin

ABSTRACT

Here we have developed a versatile liposome-mediated drug delivery system (DDS) allowing a strong bridge between the streptavidin-tagged liposome (SAL) and biotin (Bi)-tagged biomaterials which has strong affinity to surface proteins expressed in restricted cell lineages. This DDS was effective and specific for many leukemia cells *in vitro* and *in vivo*. When examining 6 human leukemia cell lines using calcein-encapsulated SALs in combination with Bi-granulocyte colony-stimulating factor (G-CSF), Bi-anti-CD33 monoclonal antibody (MAb) or Bi-anti-CD7 MAb, the fluorescent positive rate of each cell line was in almost proportion to degree of G-CSF receptor, CD33 or CD7 expression, respectively. More importantly, the binding ability was shown to be well maintained in a mouse xenograft model. Furthermore the cytosine arabinoside (AraC)-encapsulated SALs could kill the corresponding cells much more effectively in combination with Bi-biomaterials than free AraC, as expected. These findings strongly indicate that our SAL/Bi-biomaterial system could allow various types of medical agents to be delivered reliably and stably to the cells targeted.



## 1. Introduction

For better diagnosis and treatment, highly efficient and specific delivery systems of various medical agents to particular cell types, including leukemia cells, become more and more required. Concerning to anti-cancer agents, introduction of immunoliposome using monoclonal antibodies (MAbs) for specific cell targeting seems to satisfy these requirements to some degree in various cancers (Eliaz and Szoka, 2001; Maruyama, 2002; Park et al., 2002), and also its application range would be expected to expand by using natural ligands instead of MAbs. To date, MAb against HER2 (Park et al., 2002), or transferring receptors (Xu et al., 2002), folate (Pan et al., 2002), CD44 (Eliaz and Szoka, 2001), and CD74 (Hertlein et al., 2010) have been used as the attachment of the immunoliposomes. However, some problems still remain to be solved. They include binding weakness between liposomes and antibodies or ligands, and between target cells and antibodies or ligands, which structural changes and destruction of MAbs or ligands caused by oxidation/reduction stress and proteolysis are responsible. In order to protect MAbs or ligands from such attacks, we applied the strong affinity between streptavidin (SA) and biotin (Bi) (Diamandis and Christopoulos, 1991), the efficacy of which has been demonstrated in clinical trials as specific radioimmunotherapy (Knox et al., 2000; Weiden et al., 2000). Thus in our system, liposomes were tagged with SA (SAL), while MAbs or ligands with Bi. Here we show the results strongly suggesting that our newly developed liposome-mediated drug delivery system (DDS) would be used effectively to develop *in vitro* and *in vivo* diagnostic and therapeutic agents, particularly for leukemias.

## 2. Materials and methods

### 2.1. Cell lines

The human leukemia cell lines used in this study were acute myeloid leukemia (AML) cell lines Kasumi-1 (Asou et al., 1991) and

* Corresponding author at: Department of Chemistry/Biological Chemistry, School of Science and Engineering, Waseda University, 3-4-1, Okubo, Shinjuku-ku, Tokyo 169-8555, Japan. Tel.: +81 3 5286 8220; fax: +81 3 5286 8227.
*E-mail address:* asgtkmd@waseda.jp (S. Asano).
[1] Both these authors contributed equally to this work.

0378-5173/$ – see front matter © 2013 Published by Elsevier B.V.
http://dx.doi.org/10.1016/j.ijpharm.2013.06.031

IMS-M2 (Setoyama et al., 1998), chronic myeloid leukemia blast crisis (CML-BC) cell lines MEG-01 and K562 (provided by American Type Culture Collection (ATCC), Rockville, MD, USA), T-cell acute lymphoblastic leukemia (T-ALL) cell line Jurkat (provided by ATCC) and Philadelphia Chromosome positive ($Ph^+$) ALL cell line KOPN-30 (kindly provided by Drs. K. Sugita and S. Nakazawa, Yamanashi University, Yamanashi, Japan) (Drexler et al., 2000; Drexler and Minowada, 1998). All of those cell lines were cultured in RPMI 1640 medium supplemented with 10% fetal bovine serum (FBS) at 37 °C with a humidified atmosphere of 5% $CO_2$.

### 2.2. Preparation of SALs

1,2-Distearoyl-sn-glycero-3-phosphoethanolamine-N-[maleimide (polyethylene glycol) (DSPE-PEG-Mal) with 2000 in average molecular weight of polyethylene glycol, was purchased from Avanti Polar Lipids (AL, USA). PEG-liposomes were composed of dipalmitoyl phosphatidylcholine (DPPC), cholesterol (CH) and DSPE-PEG-Mal (2:1:0.06 m/m). PEG-liposomes containing calcein (Dojindo Laboratories, Kumamoto, Japan) or Ara-C (Nippon Shinyaku Co., Ltd. Kyoto, Japan) were prepared using reverse-phase evaporation followed by extrusion (Lipex Biomembranes, Vancouver, Canada) through 2-stacked polycarbonate membrane filters (0.1 μm pore size, Whatman, MA, USA) as described previously (Maruyama et al., 1995).

To prepare SALs, SA (ImmunoPure Streptavidin, Pierce, Rockford, IL, USA) was bound to PEG chain of the PEG-liposome surface as follows. SA was reacted in methanol with 20 mM solution of N-succinimidyl 3-(2-pyridyldithio) propionate (SPDP) (Sigma, St. Louis, MO, USA) in PBS (pH7.4), and stirred for 30 min at room temperature. The product was purified by chromatography on Sephadex G25. Ditiothleitol (DTT, Sigma, St. Louis, MO, USA) was then added to the streptavidin-SPDP, at a final concentration of 50 mM, followed by 30 min incubation, to reduce the SPDP, permitting it to react with maleimide moiety on the surface of the PEG-liposome. After separation of the product using Sephadex G25, the reduced streptavidin-SPDP was incubated with the PEG-liposomes over night at 4 °C. SALs were separated from the free SA by a Bio-Gel A-1.5m column (BioRad, Hercules, CA, USA). The average size of the liposomes used in this study was about 120 nm, and there were no significant differences in average size among all types of liposomes. The calcein-encapsulated liposomes used in this study were calcein-encapsulated PEG-liposomes without the SA (Cal-PL) and calcein-encapsulated SAL (Cal-SAL). The Ara-C-encapsulated liposomes were Ara-C-encapsulated SAL (Ara-C-SAL).

### 2.3. Analysis of surface antigens in leukemia cells

To determine the expression of CD33, CD7 or granulocyte colony stimulating factor (G-CSF) receptor (G-CSFR) on the cell surface of leukemia cells, 20 μL of 10 μg/mL of Bi-anti-CD33 MAb (Ancell, Bayport, MN, USA), 1 μg/mL of Bi-anti-CD7 MAb (ID Labs Inc., London, Ontario, Canada) or 200 ng/mL of Bi-recombinant human (rh)-G-CSF (kindly provided by Chugai Pharmaceutical Co., Ltd. Tokyo, Japan) in PBS were added to $1 \times 10^6$ cells for 30 min at 4 °C. Thereafter, cells were washed and incubated for 15 min at room temperature with phycoerythrin (PE)-conjugated SA (SA-PE) (Dako, Glostrup, Denmark). These cells were washed and fixed with 1% paraformaldehyde (PFA) in PBS. The obtained samples were analyzed by flow cytometry (FCM) with a FACS Calibur flow cytometer (Becton Dickinson, Franklin Lakes, NJ, USA).

### 2.4. Binding and internalization assay of SALs by FCM

To detect the binding of Cal-PL to target cells, cells were incubated with Bi-linkers first as described above. After washing with PBS, these cells were incubated with 20 μL of 30 μg/mL liposomes for 30 min at 37 °C and analyzed by FCM. To verify the specificity of liposome binding, cells were treated with unlabeled linkers for 30 min at 4 °C before incubation of Bi-anti-CD33 MAb. Thereafter, cells were treated with the Cal-SALs and appraised by FCM. To examine the internalization efficiency of the liposomes, $1 \times 10^6$ cells treated with Bi-linkers were incubated with Cal-SALs for 30 min at 37 °C in the presence or absence of sodium azide. Cell surface-bound liposomes were digested by incubation with 20 mg/mL pronase (Roche Diagnostics, Basel, Switzerland) for 30 min at 4 °C, and then cells were fixed and analyzed by FCM.

### 2.5. Confocal microscopy

Binding and internalization of the liposomes in target cells were also examined by confocal microscopy. Cells were incubated with Bi-linkers for 30 min at 4 °C and washed twice with PBS followed by incubation with 0.9 mg/mL Cal-SALs for 5 min or 2 h at 37 °C. These cells were attached to slide glasses by using Cytospin 3 (Shandon, Roncorn, UK) and fixed with 1% PFA solution. Thereafter, cells were incubated with 1U of rhodamine phalloidin (Molecular Probes, Eugene, OR, USA) for 15 min at room temperature to stain cytoplasmic actin followed by washing with distilled water 3 times. The prepared samples were observed with Zeiss Axioskop2 plus microscopy (Carl Zeiss, Jena, Germany). Green fluorescence of calcein and red fluorescence of rhodamine phalloidin were analyzed, and merged images were produced by using Radiance 2100 Confocal, Multi-photon Imaging Systems and LaserSharp 2000 software (Bio-Rad Laboratories, Hercules, CA, USA).

### 2.6. Cytotoxicity assay

To determine the cytotoxic effect of the Ara-C-encapsulated liposomes, leukemia cells were treated with Bi-linkers as described, and then were cultured in the presence or absence of Ara-C-SAL or free Ara-C for 48 h at 37 °C. The final concentrations of Ara-C used in this assay varied from 1 to 1000 nM. After 30 min incubation at 37 °C, cells were washed with PBS and cultured for an additional 48 h at 37 °C. The viability of cells treated with Ara-C-encapsulated liposomes was assessed by trypan blue exclusion test.

### 2.7. Animal study

Ten-week-old female NOD-SCID mice were obtained from CLEA Japan (Tokyo, Japan). The mice were maintained under specific pathogen-free conditions. Five million IMS-M2 cells were injected intravenously into the mice that had received prior irradiation of 350 cGy and injection of 100 μg anti-asialo-GM1 antibody (Wako Pure Chemical Industries Ltd., Osaka, Japan). When paralysis of the hind legs was observed, indicating systemic involvement of IMS-M2, blood was drawn and treated with Bi-anti-CD33 MAb and SA-PE to detect the circulating IMS-M2 cells by FCM. After confirmation of the engraftment, 1.5 μg of Bi-anti-CD33 MAb was first injected into the tail vein, and 450 μL of 0.09 mg/mL Cal-SALs was then injected after 15 min. After 1 h, the mice were euthanized, and blood, spleen and bone marrow cells were sampled to determine the distribution of Cal-SALs, using APC-conjugated anti-CD33 MAb (Immunotech, Inc., Westbrook, ME, USA) by FCM.

## 3. Results

### 3.1. Specific binding of SALs to leukemia cells

First, we evaluated the expression level of G-CSFR, CD33 and CD7 in the 6 leukemia cell lines listed in Table 1, using FCM. Kasumi-1 cells highly expressed G-CSFR at positive rate of 95% (Fig. 1A). CD33

Please cite this article in press as: Chen, M.-H., et al., A versatile drug delivery system using streptavidin-tagged pegylated liposomes and biotinylated biomaterials. Int J Pharmaceut (2013), http://dx.doi.org/10.1016/j.ijpharm.2013.06.031

**Table 1**
Expression of surface antigen in leukemia cell lines and binding of SALs with Bi-linkers.

| Cells | Origin | G-CSFR | | CD33 | | CD7 | |
|---|---|---|---|---|---|---|---|
| | | Exp[a] | SAL[b] | Exp | SAL | Exp | SAL |
| Kasumi-1 | AML | 95 | 87 | 99 | 97 | 0 | 0 |
| IMS-M2 | AML | 0 | 0 | 99 | 94 | 74 | 30 |
| Meg-01 | CML-BC | 0 | 0 | 99 | 99 | 0 | 0 |
| Jurkat | T-ALL | 0 | 0 | 0 | 0 | 99 | 98 |
| K562 | CML-BC | 0 | 0 | 0 | 0 | 0 | 0 |
| KOPN30 | $Ph^+$ ALL | 0 | 0 | 0 | 0 | 0 | 0 |

G-CSFR, granulocyte colony-stimulating factor receptors; AML, acute myeloid leukemia; CML-BC, chronic myeloid leukemia blast crisis; T-ALL, T-cell acute lymphoblastic leukemia; $Ph^+$ ALL, Philadelphia Chromosome positive ALL.
[a] % of Bi-linker-bound cells determined by FCM.
[b] % of Cal-SAL-bound cells determined by FCM.

was expressed strongly in the AML cell lines IMS-M2 and Kasumi-1, and the CML-BC cell line MEG-01 at a positive rate of almost 100% (Fig. 1A and Table 1). CD7 was expressed strongly in the T-ALL cell line Jurkat (99%) and moderately in IMS-M2 cells (74%) (Fig. 1A and Table 1). CML-BC K562 cells and $Ph^+$ ALL KOPN-30 cells did not express G-CSFR, CD33, or CD7 (Table 1). To evaluate the binding of SALs to these cell lines, the cells were treated with Bi-G-CSF, Bi-CD33 or Bi-CD7 followed by incubation with Cal-SALs, and analyzed by FCM. Kasumi-1 cells showed high expression of calcein when the cells were treated with Bi-G-CSF (87%) (Fig. 1B). IMS-M2, Kasumi-1 and MEG-01 cells treated with Bi-anti-CD33 MAb and Cal-SALs were strongly positive for calcein fluorescence (94%, 97%, and 99%, respectively) (Fig. 1B, Table 1). Jurkat cells and IMS-M2 cells were also positive for calcein when treated with Bi-anti-CD7 MAb (98% and 30%, respectively) (Fig. 1B, Table 1). In contrast, none of these cell lines were positive for calcein when treated with Bi-linkers for unexpressed antigens and SALs, and calcein fluorescence was not detected in K562 and KOPN-30 cells ($CD33^-CD7^-G\text{-}CSFR^-$) after treatment with any of the Bi-linkers and SALs (Table 1). In addition, the binding efficiencies of PEG-liposomes, which were not carrying SA on their surface, to those cells was much lower than those of SALs even when the Bi-linkers for positive antigens in target cells were used (data not shown). These results suggested that the specific binding of SALs to leukemia cells is mediated by binding of the Bi-linkers to cell surface antigens. To confirm this point, a competition assay was performed. The binding of Cal-SALs to IMS-M2 cells *via* Bi-anti-CD33 MAb was inhibited by addition of unlabeled anti-CD33 MAb in a dose-dependent manner (Fig. 1C). Similar results were obtained in Kasumi-1 and Jurkat cells when unlabeled

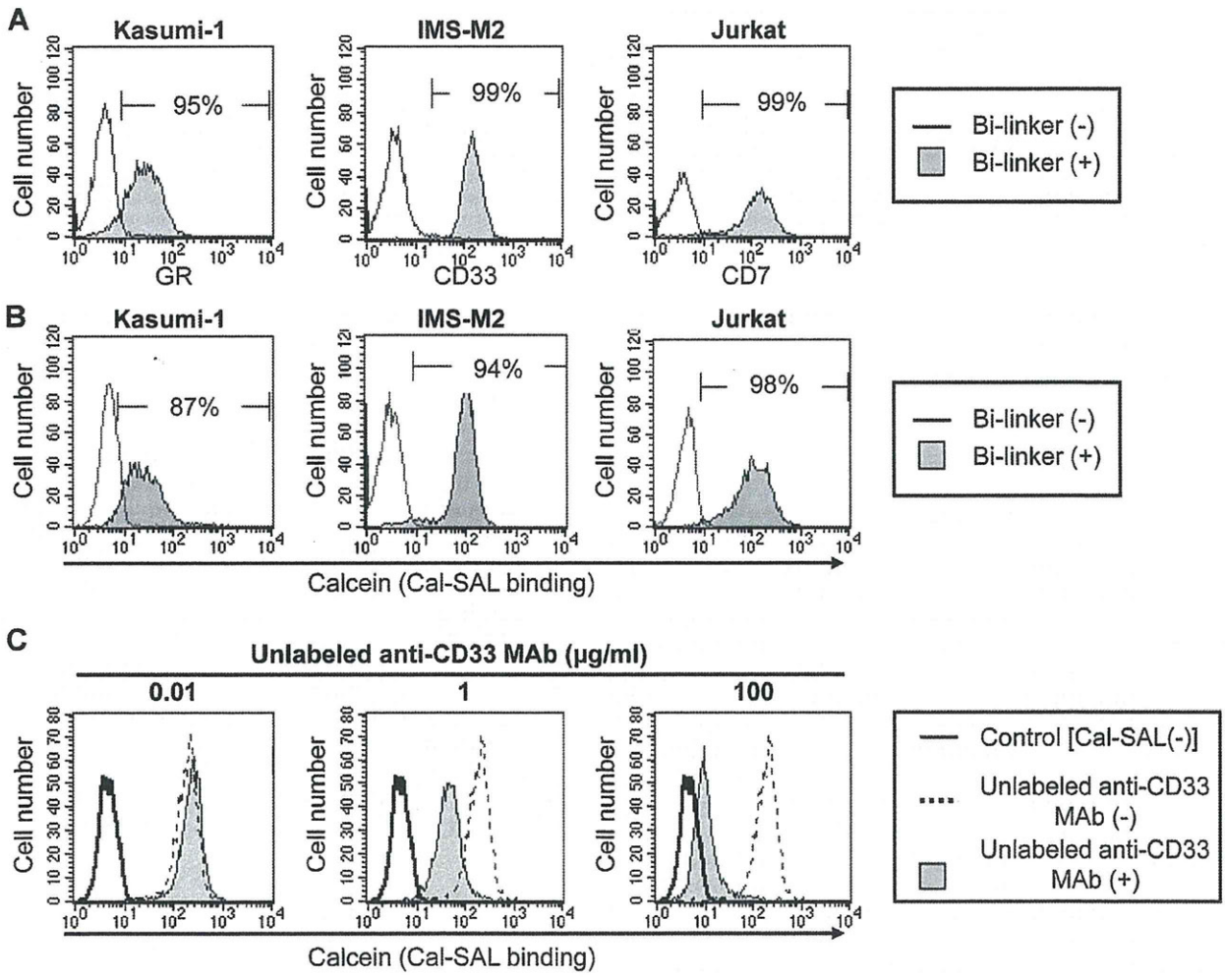


**Fig. 1.** Expression of G-CSF receptor (GR), CD33 or CD7 and binding of Calcein-encapsulated streptavidin liposomes (Cal-SALs) to leukemia cell lines. (A) Expression of GR, CD33 or CD7 to leukemia cell lines Kasumi-1, IMS-M2 and Jurkat cells treated with biotinylated (Bi-) G-CSF (Bi-G-CSF), Bi-anti-CD33 MAb and Bi-anti-CD7 MAb, respectively, were determined by FCM. (B) Cal-SAL binding to these cells was also determined by FCM. (C) Inhibition of Cal-SAL binding to IMS-M2 cells by unlabeled anti-CD33 MAb. IMS-M2 cell lines were pre-pretreated with various concentration of unlabeled anti-CD33 MAb and then incubated with Bi-anti-CD33 MAb. Thereafter, cells were treated with Cal-SALs and analyzed by FCM.

Please cite this article in press as: Chen, M.-H., et al., A versatile drug delivery system using streptavidin-tagged pegylated liposomes and biotinylated biomaterials. Int J Pharmaceut (2013), http://dx.doi.org/10.1016/j.ijpharm.2013.06.031

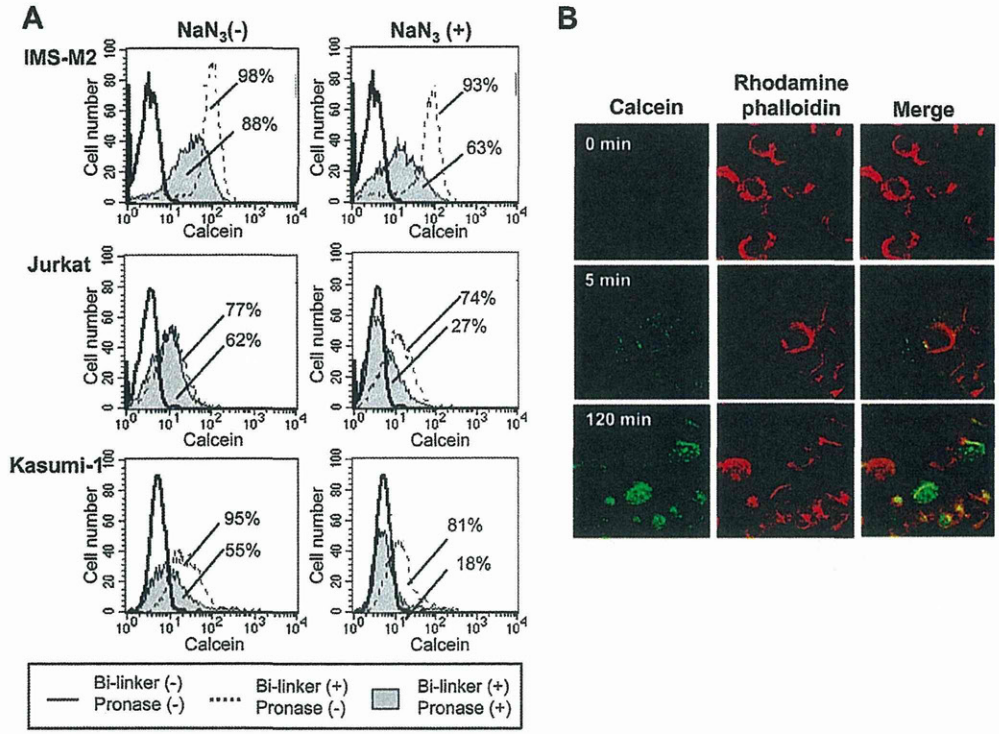


**Fig. 2.** Internalization of Cal-SALs into leukemia cells. (A) Flow cytometry of leukemia cells treated with Cal-SALs and corresponding Bi-ligands. Cells were pretreated with indicated Bi-ligands and incubated with Cal-SALs in the absence (left panel) or presence (right panel) of sodium azide ($NaN_3$). The fluorescence intensity of calcein was evaluated after treatment with (gray area) or without (broken line) pronase. The cells treated with the CAL-SALs but not with the corresponding Bi-ligands were used as a negative control (solid line). IMS-M2 cells with Bi-anti-CD33 MAb, Jurkat cells with Bi-anti-CD7 MAb, Kasumi-1 cells with Bi-G-CSF. (B) Internalization analysis of Cal-SALs by laser-scanning confocal microscopy. Jurkat cells were incubated with Bi-anti-CD7 MAb for indicated times followed by incubation with Cal-SALs. The cells were stained with rhodamine phalloidin to visualize cytoplasmic actin. Green fluorescence of calcein (left column), red fluorescence of rhodamine phalloidin (center column), and the merged image (right column) are shown. Localization of Calcein signals in cytoplasm is detected after 120 min incubation. Color images are available in the web version of this article.

G-CSF and anti-CD7 MAb was added, respectively (data not shown). These results indicated the specific binding of SALs through binding of Bi-linkers to surface antigens.

### 3.2. Internalization of SALs in leukemia cells

To determine the internalization efficiencies of SALs with Bi-linkers into targeted cells, these cells were analyzed by FCM in the presence or absence of sodium azide and/or pronase. Pre-treatment of cells with sodium azide blocks internalization of cell surface antigens, and post-treatment with pronase detaches the liposomes from the cell surface if the liposomes are not internalized. Internalization efficiencies of Cal-SALs can be measured by comparing of the percentage of pronase-resistant fluorescence intensity between the presence and absence of sodium azide. In this study, after pronase treatment in the sodium azide pretreated condition, the fluorescence intensity was significantly reduced in IMS-M2, Jurkat and Kasumi-1 cells that were treated with Cal-SALs and Bi-linkers. In contrast, the reduction of the fluorescence intensity of those cells after pronase treatment was less in the sodium azide-untreated condition than in the sodium azide-treated condition (Fig. 2A). These results strongly suggested that the SALs were not only bound to the cell surface but also internalized into the cytoplasm in the absence of sodium azide. To confirm the internalization of the SALs, Jurkat cells treated with Bi-anti-CD7 MAb and Cal-SALs were observed by confocal microscopy. Calcein fluorescence was detected only on the cell surface 5-min after incubation, and was detected in the cytoplasm 2-h after incubation, indicating the internalization of SALs into cytoplasm (Fig. 2B). In other cell lines treated with Bi-anti-CD33 MAb or Bi-G-CSF, similar results were obtained (data not shown).

### 3.3. Effect of Ara-C-SALs on leukemia cell lines

To determine whether the SAL-based DDS is useful for tumor killing, the three leukemia cell lines were cultured with various concentrations of Ara-C-SALs or uncapsulated Ara-C (free Ara-C) for 48 h, and numbers of living cells were analyzed. Ara-C-SALs reduced cell numbers more effectively in IMS-M2, Jurkat and Kasumi-1 cells than free Ara-C when these cells were treated with Bi-anti-CD33 MAb, Bi-anti-CD7 MAb and Bi-G-CSF, respectively (Fig. 3). The $IC_{50}$ of the Ara-C-SALs combined with Bi-linkers was significantly lower than that of the free Ara-C. The difference of $IC_{50}$ between Ara-C-SALs and free Ara-C were 12.7-fold, 13.4-fold and 2.1-fold for IMS-M2 cells treated with Bi-anti-CD33 MAb, Jurkat cells with Bi-anti-CD7 MAb, and Kasumi-1 cells with Bi-G-CSF, respectively (Table 2). In contrast, the inhibitory effect of the SALs on those cells was weaker in the absence of those Bi-linkers than in their presence (Fig. 3), and $IC_{50}$ of the SALs without Bi-linkers was much higher

**Table 2**
$IC_{50}$ [nM] of Ara-C-SALs in leukemia cell lines.

| Treatment | IMS-M2 | Jurkat | Kasumi-1 |
|---|---|---|---|
| | Bi-anti-CD33 MAb | Bi-anti-CD7 MAb | Bi-G-CSF |
| Free Ara-C | 92.5 ± 17.2 | 85.7 ± 15.3 | 68.3 ± 6.8 |
| Ara-C-SAL [Bi-linker (+)] | 7.3 ± 2.0 | 6.4 ± 0.6 | 31.8 ± 1.0 |
| Ara-C-SAL [Bi-linker (-)] | 83.4 ± 3.0 | 72.6 ± 4.1 | 57.7 ± 3.8 |

Bi-linker, biotinylated linker; SAL, streptavidin-liposome.

Please cite this article in press as: Chen, M.-H., et al., A versatile drug delivery system using streptavidin-tagged pegylated liposomes and biotinylated biomaterials. Int J Pharmaceut (2013), http://dx.doi.org/10.1016/j.ijpharm.2013.06.031

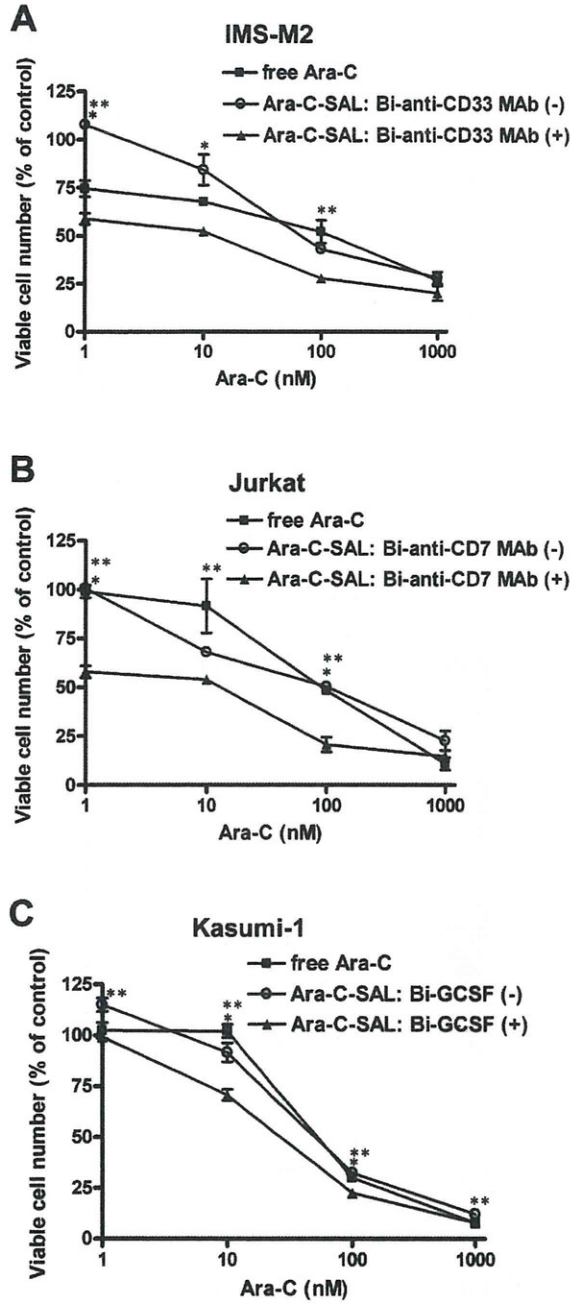


**Fig. 3.** Viability of leukemia cell lines treated with Ara-C-containing SALs (Ara-C-SALs) and Bi-ligands. Cells were incubated with Ara-C-SALs or free Ara-C with or without treatment of Bi-ligands, and live cell numbers were counted. The final concentrations of Ara-C varied from 1 to 1000 nM. (A) IMS-M2 cells with Bi-anti-CD33 MAb. (B) Jurkat cells with Bi-anti-CD7 MAb. (C) Kasumi-1 cells with Bi-G-CSF. Data represents mean ± SD of triplicate experiments and is statistically analyzed with the Student's *t*-test. $^{*}p < 0.05$, free Ara-C *vs.* Ara-C-SALs with Bi-ligands; $^{**}p < 0.05$, Ara-C-SALs without Bi-ligands *vs.* Ara-C-SALs with Bi-ligands.

than that with Bi-linkers and almost same as that of free Ara-C. These results suggested that this SAL-mediated DDS is useful for targeting leukemia cells.

### 3.4. *In vivo* binding of SALs

To evaluate the targeting ability of our SAL-mediated DDS system *in vivo*, the distribution of the Cal-SALs in NOD-SCID mice that transplanted with IMS-M2 cells was determined. Four weeks after transplantation, engrafted IMS-M2 cells were detected in the peripheral blood by FCM (Fig. 4 A). Because the anti-CD33 MAb used in this assay was human-specific, all $CD33^{+}$ cells were the grafted IMS-M2 cells. We injected the Bi-anti-CD33 MAb intravenously followed by injection of the SALs, and 1 h after injection of the injection, PB, spleen and BM cells were sampled and analyzed by FCM. Most of leukemia cells from PB and the spleen, and some leukemia cells from BM were calcein-positive (Fig. 4B–D). However, we could not detect the calcein fluorescence in the mouse cells, which were negative for human CD33. These results demonstrated that the SALs could bind to leukemia cells specifically with the Bi-anti-CD33 MAb not only *in vitro*, and should be *in vivo*.

## 4. Discussions

To improve the clinical outcome of leukemia patients, dose escalation of chemotherapeutic agents has been tried, because insufficient dose of anti-tumor drugs may lead to a high incidence of relapse and drug resistance. However, many patients suffer from various side effects during high-dose chemotherapy, which limits its application extensively (Ahmad et al., 1993). To avoid these problems, tumor-specific therapy is thought to be promising, and drugs targeting oncogene products or a specific delivery system to tumor cells have been developed vigorously (Minko et al., 2004; Rowlinson-Busza and Epenetos, 1992). Encapsulation of cytotoxic drugs in liposomes is thought to be an excellent procedure in this regard, because liposomes are able to transfer and penetrate into tumor tissues more preferentially than into normal tissues (Allen, 1997; Pea et al., 2000). Consequently, many types of liposomes containing cytotoxic agents have been developed for many kinds of solid cancers (Jiang et al., 2013; Maruyama, 2002; Sugano et al., 2000). On the other hand, only a few reports have described the development of liposomes for leukemia, and the enhanced permeability and retention effect would not be expected in leukemia. Recently, immunoliposomes, one kind of ligand-mediated targeting DDS, which are attached to the liposome surface with ligands of surface antigens in target cells, have been developed to achieve tumor cell-specific delivery (Maruyama, 2002; Sapra and Allen, 2003). We previously reported that imatinib-encapsulated immunoliposomes using anti-CD19 MAb killed Philadelphia chromosome-positive ALL cells efficiently, indicating the immune-liposome system useful (Harata et al., 2004).

Our system presented here should satisfy the following requirements: drug in liposomes should be delivered to target cells selectively with specific ligands and then internalized by target cells, making high intracellular drug concentration (Allen, 2002; Maruyama, 2011). To achieve these aims, several considerations should be taken. First, target antigen or receptors must overexpress on target cells and provide sufficient binding ability to its receptor. In this study, G-CSFR was considered to be a good candidate to target myeloid cells, including the AML cells of many patients, but not normal uncommitted hematopoietic stem cells (HSCs) (Tsuji and Ebihara, 2001). We considered that direct coupling of G-CSF and liposomes might result in loss of binding ability of G-CSF due to conformational change by cutting the internal disulfide bond (Haniu et al., 1996). Therefore, we have developed an indirect coupling system using SALs and Bi-linkers to maintain binding ability of G-CSF. These results encouraged us to demonstrate the versatility of our SAL-based DDS. For this purpose, CD33 and CD7 were chosen as the target antigens because of expression range of these antigens. CD33 is expressed in myeloid-committed cells including myeloid leukemia cells in many cases (Simmons and Seed, 1988; van Der Velden et al., 2001), and CD7

Please cite this article in press as: Chen, M.-H., et al., A versatile drug delivery system using streptavidin-tagged pegylated liposomes and biotinylated biomaterials. Int J Pharmaceut (2013), http://dx.doi.org/10.1016/j.ijpharm.2013.06.031